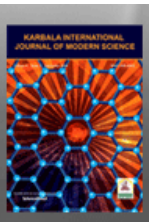

Karbala International Journal of Modern Science

Volume 8 | Issue 1 Article 7

Simulation and Improvement of the Efficiency of the CFTS Solar Cell Using SCAPS-1D

Hardan T. Ghanem Dr.
Department of physics, College of Education for Pure Science, Tikrit University, Iraq, hardanganem@gmail.com

Ayed N. Saleh
Department of physics, College of Education for Pure Science, Tikrit University, Iraq

Muaamer A. Kamil
Department of physics, College of Education for Pure Science, Tikrit University, Iraq

Follow this and additional works at: https://kijoms.uokerbala.edu.iq/home

 Part of the Biology Commons, Chemistry Commons, Computer Sciences Commons, and the Physics Commons

Recommended Citation

Ghanem, Hardan T. Dr.; Saleh, Ayed N.; and Kamil, Muaamer A. (2022) "Simulation and Improvement of the Efficiency of the CFTS Solar Cell Using SCAPS-1D," *Karbala International Journal of Modern Science*: Vol. 8 : Iss. 1 , Article 7.
Available at: https://doi.org/10.33640/2405-609X.3207

This Research Paper is brought to you for free and open access by Karbala International Journal of Modern Science. It has been accepted for inclusion in Karbala International Journal of Modern Science by an authorized editor of Karbala International Journal of Modern Science. For more information, please contact abdulateef1962@gmail.com.

University of Kerbala

Simulation and Improvement of the Efficiency of the CFTS Solar Cell Using SCAPS-1D

Abstract

A simulation of the AZO/i-ZnO/CdS/CFTS solar cell was carried out using SCAPS software. The results were obtained (Voc=0.55 V, Jsc=6.2 mA/cm^2, FF=39 %, η=1.35 %). Simulation results were compared with experimental research and we got convergence in the results (Voc=0.56 V, Jsc=6.5 mA/cm^2, FF=37 %, η=1.37 %). The simulated solar cell is improved by increasing the doping concentration and thickness of the buffer and absorption layers. The efficiency of the solar cell was improved to η=4.29%, fill factor FF=52.92%, open circuit voltage Voc=0.74 V and short circuit current Jsc=10.8 mA/cm^2

Keywords

SCAPS, Solar cells, Simulation solar cells, CFTS

Creative Commons License

This work is licensed under a Creative Commons Attribution-Noncommercial-No Derivative Works 4.0 License.

This research paper is available in Karbala International Journal of Modern Science: https://kijoms.uokerbala.edu.iq/home/vol8/iss1/7

RESEARCH PAPER

Simulation and Improvement of the Efficiency of the CFTS Solar Cell Using SCAPS-1D

Hardan T. Ganem*, Ayed N. Saleh, Muaamar A. Kamil

Department of Physics, College of Education for Pure Science, Tikrit University, Tikrit, Iraq

Abstract

A simulation of the AZO/i-ZnO/CdS/CFTS solar cell was carried out using SCAPS software. The results were obtained (Voc = 0.55 V, Jsc = 6.2 mA/cm^2, FF = 39%, η = 1.35%). Simulation results were compared with experimental research and we got convergence in the results (Voc = 0.56 V, Jsc = 6.5 mA/cm^2, FF = 37%, η = 1.37%). The simulated solar cell is improved by increasing the doping concentration and thickness of the buffer and absorption layers. The efficiency of the solar cell was improved to η = 4.29%, fill factor FF = 52.92%, open circuit voltage Voc = 0.74 V and short circuit current Jsc = 10.8 mA/cm^2.

Keywords: SCAPS, Solar cells, Simulation solar cells, CFTS

1. Introduction

Fossil fuels are nowadays the main source of energy that is consumed all over the world. In 2015 the world's total energy consumption is 647.13 Mtoe and more than 86% of that energy is on fossil and nuclear fuels. But fossil fuels are resource-limited and create pollution by emitting carbon dioxide and impurities from Arsenic and other heavy metals that are harmful to human health [1].

In the wake of the industrial revolution and technological development, digital technology topped the scene, and scientists kept looking into the extent to which it simulated the experimental reality, so much software was invented and included in the research arena due to the increasing need for energy and the depletion of its stock and to find alternative sources of energy, and the most important alternative sources of energy are solar cells. So, it has cleared that low coast and environmentally friendly, but low efficiency and needs large areas, which called on researchers to increase the study on these cells to get the best results. Semiconductors absorb photons that have an energy greater than the forbidden energy gap and lose the excess energy by thermal, radiative, or non-radiative processes, and there are efforts to increase their efficiency by achieving the manufacture of various solar cells [2]. In the past, science and technology had a huge impact on our society. Which helped in the comprehensive understanding of materials and electronics that led to the increase of inventions and progress [3], One of the successful techniques for manufacturing thin films for solar cells, which achieved good results, is the compounds CdTe and CIGS, but Cd is a toxic element in nature, as well as the elements Te, In and Ge are not available, so they are expensive, so the research continues to find a successful alternative [4]. We show that the compound CZTS, one of the important compounds due to its membranes, is low-toxic and available in the earth's crust and has a relatively high efficiency of about 12.7%, and has an energy gap of 1.5 eV [5]. The conversion efficiency of CZTS reached about 10% [6,7] which is larger than the efficiency of CIGS, which amounted to about 7.21% [8]. Note that it is less than the optimal efficiency on the Queasier Shockley limit, which amounted to 28% [9]. It is still not possible to achieve a conversion efficiency of 28% in

Received 17 September 2021; revised 7 December 2021; accepted 8 December 2021.
Available online 11 February 2022

* Corresponding author at:
E-mail addresses: hardanganem@gmail.com (H.T. Ganem), ayed.ns@tu.edu.iq (A.N. Saleh), muaamar.a.kamil@tu.edu.iq (M.A. Kamil).

https://doi.org/10.33640/2405-609X.3207
2405-609X/© 2022 University of Kerbala. This is an open access article under the CC-BY-NC-ND license (http://creativecommons.org/licenses/by-nc-nd/4.0/).

solar cells due to the lack of understanding of the properties of semiconductor materials, Because of the chemical and compositional similarities, a continuous series of Si(oP_{32})-Ge(oP_{32}) solid solutions can be assumed. The expected band gap value of Eg = 1.361 eV for Si(oP_{32}) is very close to the Shockley–Queisser limit and indicates that silicon modification is a promising material for efficient solar cells [10]. Numerical analysis plays an important role in understanding the materials. $CuFeSnS_4$ quaternary compound (CFTS) attracted the interest of many researchers for the manufacture of solar cells due to its nontoxic elements, its abundance in the earth's crust, and its relatively large energy gap (1.2–1.8 eV) [11]. It can be prepared in many ways, including thermal chemical spraying, vacuum evaporation, rotational coating, and other methods. It is a quaternary dump that has p-type conductivity and has two types of crystal structure [12,13]. In this research, we will study the CFTS quadrupole by using numerical modeling using the SCAPS program. Numerical modeling or simulation are important methods that save us time and reduce material costs. We will discuss experimental research previously published and enhance the performance of the solar cell by addressing several things, including:

- Compare the experimental cell with the simulation cell.
- Improving the cell by changing the accepter and thickness of the absorbent layer.
- Change the donor and thickness of the buffer layer for best results.
- Compare the results after optimization with the theoretical and experimental cells.

2. Modeling

2.1. The Cell Structure

The AZO/i-ZnO/CdS/CFTS/Mo solar cell consists of three layers, first, the AZO/i-ZnO window layer has a relatively large energy gap to allow the light radiation to enter the other layers, and then the second layer CdS buffer layer has an energy gap and the medium value of electron affinity of To increase the access of photons to the absorption layer due to reducing the surface defects between the window and the absorption layers [14] and finally the third layer CFTS absorption layer possesses p-type conductivity, small energy gap, and high absorption coefficient to convert maximum energy from light to electrical energy and there is flat ohmic contact In front of me and Schottky back contact of Mo metal and have a working function of 4.6 V [15]. The cell also has a series resistance of 16.8 Ω cm^2 and a parallel resistance of 253.1 Ω cm^2 [16]. Fig. 1 shows the structure of the cell.

2.2. Numerical simulation

Simulation is an imitation of a virtual or a real system using a computer through mathematical equations. We will perform the modeling using the SCAPS program. It is a one-dimensional solar cell simulation program that was designed at the University of Ghent in Belgium to simulate traditional crystalline materials for semiconductors such as CIGS, CdTe, or other materials such as SnS, the user can describe a cell with a maximum of seven layers for different properties such as optical absorption, thickness, doping concentration, energy bandgap, and others. To determine the spectral responses. And it can be calculated in the dark and the light as a function of temperature, this program has been developed and applied to all solar cells. It is a freely available program [17] and the program depends on solving semiconductor equations. We start writing Poisson's equation [18].

$$\nabla(E) = \frac{9}{\epsilon}\left(P - n + N_D^+ - N_A^-\right) \tag{1}$$

where E is the electric field, q is the amount of charge, p is the concentration of holes, n is the concentration of electrons, ϵ is the relative permittivity, N_D is the donor concentration, N_A is the acceptor concentration.

Continuity equations are important equations and are given by [19].

$$\frac{dn}{dt} = \frac{J}{q}(\nabla(J_n) + G_n - R_n \tag{2}$$

$$\frac{dp}{dt} = \frac{J}{q}\left(\nabla\left(J_p\right) + G_p - R_p\right) \tag{3}$$

where J_n is the current density of electrons, J_p is the hole current density, G_n is the rate of generating electrons, G_p is the rate of generating holes, R_n is the rate of recombination of electrons, R_p is the rate of

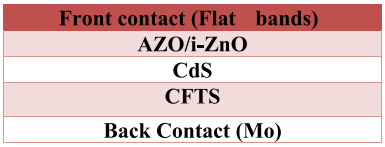

Fig. 1. The cell structure.

recombination of holes, and finally the charge carrier equations for the diffusion and drift current density and we can get them from the following equations [20].

$$J_n = q(\mu_n nE + D_n \nabla_n) \tag{4}$$

$$J_p = q\left(\mu_p nE + D_p \nabla_p\right) \tag{5}$$

where D_n is the diffusion constant for electrons, D_p is the diffusion constant for holes, μ_n is the mobility of electrons, and μ_p is the mobility of holes.

To measure the quality of photovoltaic cells, it is necessary to know the fill factor FF, the short circuit current Jsc, the open-circuit voltage Voc, and the conversion efficiency η, as these variables are related to each other by the following equations [20].

$$FF = \frac{P_{max}}{P_t} = \frac{V_{\max .Imax}}{Voc\,.\,J_{sc}} \tag{6}$$

$$\eta = \frac{P_m}{P_{in}} = \frac{Voc.Jsc\,.\,FF}{P_{in}} \tag{7}$$

where p is the electrical capacity.

And is minority carrier lifetime (τ), which is the average time required to recombine the minority carriers and is related to the defect concentration N_t and the recombination $R_{n,p}$ by the following relationship [17].

The quantum efficiency plays a distinctive role in determining the parameters of the output of solar cells. The quantum efficiency Q_E is defined as the number of electron–gap pairs generated when light falls on the pair. The following equation

$$\tau = \frac{1}{\sigma V_{th} N_t} \tag{8}$$

$$\tau = \frac{\Delta n}{R_{n,p}} \tag{9}$$

where V_{th} is the thermal velocity, σ is the electrical conductivity, Δn is the difference in the concentration of minority carriers and Table 1 shows the parameters that were used in the program.

Can be written to find the quantum efficiency [21].

$$Q_E = 1.24\,\frac{R_\lambda}{\lambda} \tag{10}$$

where Rλ is the spectral response, λ is the wavelength.

3. Discussing the results

3.1. Comparing the experimental results with the simulation results

To verify the validity of the program, experimental results were compared with theoretical

Table 1. Physical parameters of the various layers.

Parameters	symbol (unit)	CFTS	CdS	i-ZnO	AZO	Defects CFTS/CdS	Defects CFTS
Thickness	W(μm)	0.4 [16]	0.05	0.05	0.2		
Bandgap	Eg (eV)	1.87 [16]	2.4 [16]	3.3 [23]	3.3 [23]		
Electron affinity	χ (eV)	3.3 [22]	4.2 [23]	4.4 [23]	4.4 [23]		
Dielectric permittivity	ϵ	9 [22]	10 [23]	9 [24]	9 [25]		
CB effective density of states	N_C (cm^{-3})	2.2 × 10^{18} [22]	2.2 ×10^{18} [23]	2.2 ×10^{18} [24]	2.2 ×10^{18} [25]		
VB effective density of states	N_V (cm^{-3})	1.8 ×10^{19} [22]	1.8 ×10^{19} [23]	1.8 ×10^{19} [24]	1.8 ×10^{19} [25]		
Electron thermal velocity	V_n (cm/s)	1.0 ×10^7 [22]	1.0 ×10^7 [23]	1.0 ×10^7 [24]	1.0 ×10^7 [25]		
Hole thermal velocity	V_P (cm/s)	1.0 ×10^7 [22]	1.0 ×10^7 [23]	1.0 ×10^7 [24]	1.0 ×10^7 [25]		
Electron mobility	μ_n ($cm^2/v.\ s$)	21.98 [22]	100 [23]	100 [24]	100 [25]		
Hole mobility	μ_p ($cm^2/v.\ s$)	21.98 [22]	25 [23]	25 [24]	25 [25]		
Shallow uniform donor density	N_D ($1/cm^3$)	0	a variable	1.0 × 10^{14}	1.0 × 10^{20}		
Shallow uniform acceptor density	N_A ($1/cm^3$)	a variable	0	0	0		
Coefficient absorption	α (1/cm)	5.0 ×10^4 [4]	scaps	scaps	1.0 × 10^{-4}		
Capture cross section area of electrons and holes	δ_e (cm^2)					1 × 10^{-19}	× 10^{-15}
Energy level with respect to reference	Et (eV)					0.6	0.6
Total density	Nt (cm^{-2})					1.0 × 10^{13}	× 10^{-18}

Table 2. Experimental and theoretical cell outputs.

Cell structure	Voc (v)	Jsc (mA/cm^2)	FF	η
AZO/i-ZnO/CdS/CFTS/Mo (experimental)	0.56	6.5	37	1.37
AZO/i-ZnO/CdS/CFTS/Mo (theriacal)	0.55	6.2	39	1.35

results by taking layers similar to the experimental research layers and including all parameters of experimental research [16]. It was found that the theoretical results in the SCAPS program matched the results of the experimental research to a large extent, and it helped us to match the results by introducing surface defects between the absorption and buffer layer CFTS/CdS and introducing defects to the absorption layer CFTS. Table 2 shows the results of cell parameters for theoretical and experimental research. Fig. 2 shows the relationship of current with voltage. When the defects N_t increase, the conformity of the experimental work with the theoretical one increases, because of the decrease in the minority carrier lifetime, which is inversely proportional to the defects, as shown in Eq. (8), so the recombination will increase and as indicated by Eq. (9), the efficiency of the theoretical cell is less than that of the experimental cell.

3.2. The effect of the defects (N_t) of the CFTS absorption layer

Reduce the defects of the absorption layer from 10^{18} cm^{-3} to 10^{14} cm^{-3}. It turns out that the decreasing of defects increases the efficiency of the cell, so it turns from 1.35 to 1.71, but we note the stability of the parameters of the cell less than 10^{14} cm^{-2} and Fig. 3 shows the current as a function of the cell voltage with the presence of defects and the absence of defects, so the efficiency is higher when the defects decrease because reducing defects increases the life of the minority carriers, which

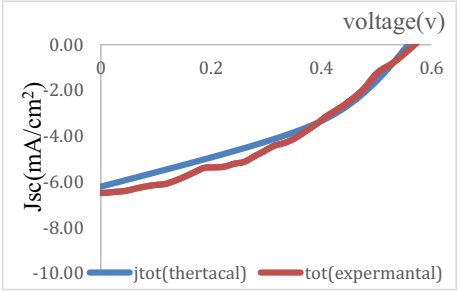

Fig. 2. The current is a function of voltage for the experimental and theoretical cells.

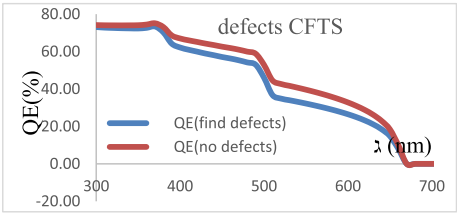

Fig. 3. The current is a function of the cell voltage with and without defects.

leads to less recombination as shown in the Eq. (8) and (9). Fig. 4 also shows the quantum efficiency as a function of the wavelength, and the little improvement appears after the decrease in the percentage of defects because the decrease in defects reduces the number of trips, which increases the widening of the energy gap, and the wavelength decreases, so the quantitative efficiency increases according to Eq. (10). Fig. 5 shows the features of the cell with different concentrations of defects in the absorption layer. We note that the decrease in the concentration of defects increases the performance of the cell.

3.3. Concentration effect of doping

3.3.1. Effect of donors (N_D) on CdS

The increase in the donor concentration increases the efficiency of the cell and the doping concentration has been changed from 10^{14} $cm^{-3}$to 10^{19} $cm^{-3}$and 10^{19} $cm^{-3}$was the best. The reason was declared before. Fig. 6 shows the relation between current and voltage in dopant concentration. And the Fig. 7 finds out the relation of the quantum efficiency with the wavelength varies with the concentration of the doping. We notice an increase in the quantitative efficiency with an increase in the donor concentration, due to the increase in the spectral response, which is directly proportional to the quantitative efficiency, as shown in Eq. (10). Fig. 8 shows that the increase in doping leads to an increase in all cell parameters.

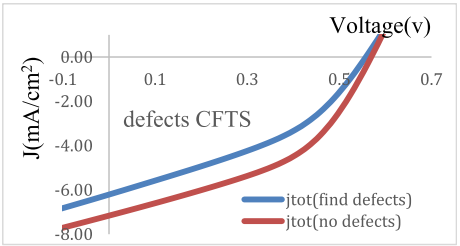

Fig. 4. Quantitative efficiency is a function of the wavelength of the cell with defects and without defects.

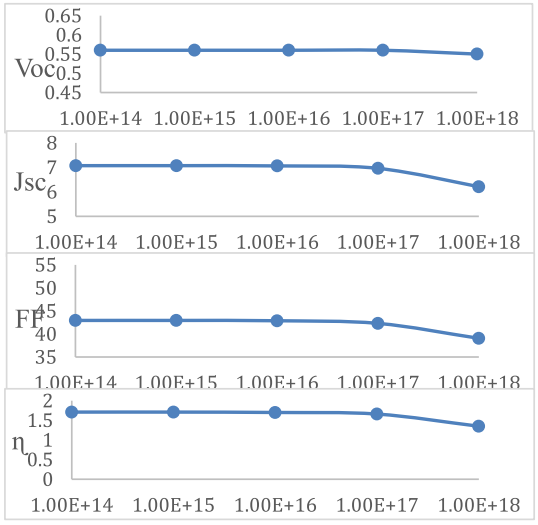

Fig. 5. Cell parameters as a function of concentration defects with of absorption layer.

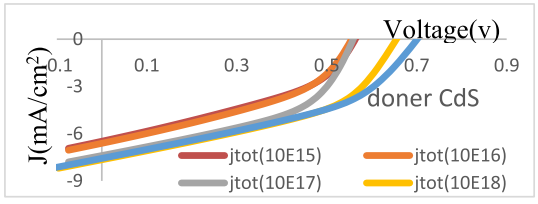

Fig. 6. Current as a function of voltage for different thickness values of the buffer layer.

3.3.2. Effect of acceptors (N_A) on CFTS

The doping concentration of the accepter layer was increased from 10^{14} cm^{-3} to 10^{18} cm^{-3} and the cell efficiency increased and became 2.45%. Fig. 9 shows the relation between the current and voltage at different doping values and the best doping concentration was 10^{18} cm^{-3} because the concentration decreasing leads to decreasing the density and saturation current, so the open-circuit voltage increases [26]. In Fig. 10, the relationship of efficiency with wavelength is shown. We notice that the quantum efficiency decreases with increasing the concentration, and the reason is that the increase in

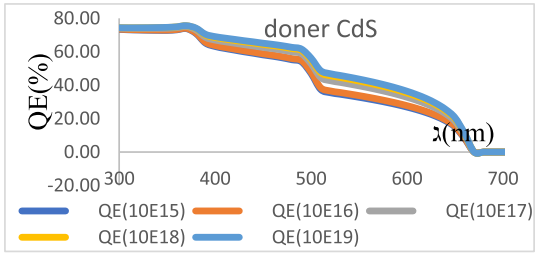

Fig. 7. Quantitative efficiency as a function of wavelength for different values of doping of the buffer layer.

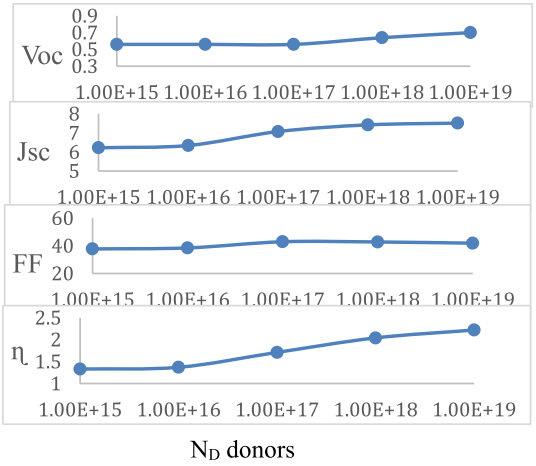

Fig. 8. Cell parameters as a function of doping concentration of the CdS layer.

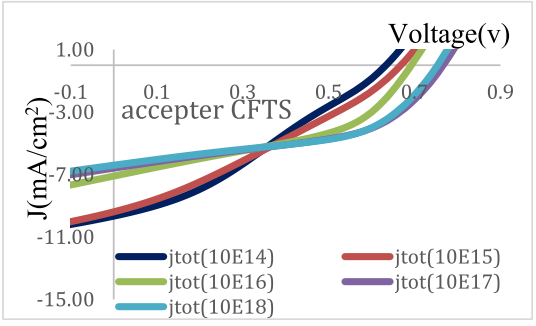

Fig. 9. Current as a function of voltage for different doping values of the absorption layer.

doping increases the number of traps, so the energy gap decreases, which leads to an increase in the wavelength, so the quantitative efficiency decreases according to Eq. (10). Fig. 11 shows the increase in cell parameters with increasing doping concentration.

3.4. W_t the thickness effect

3.4.1. Thickness of CFTS

We changed the thickness and noticed an increase in the cell performance when increasing the

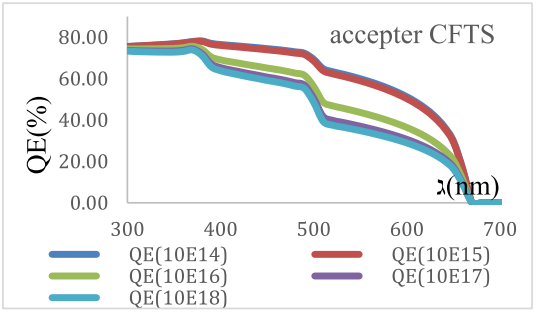

Fig. 10. Quantum efficiency as function wavelength for different values concentration doping layer absorption.

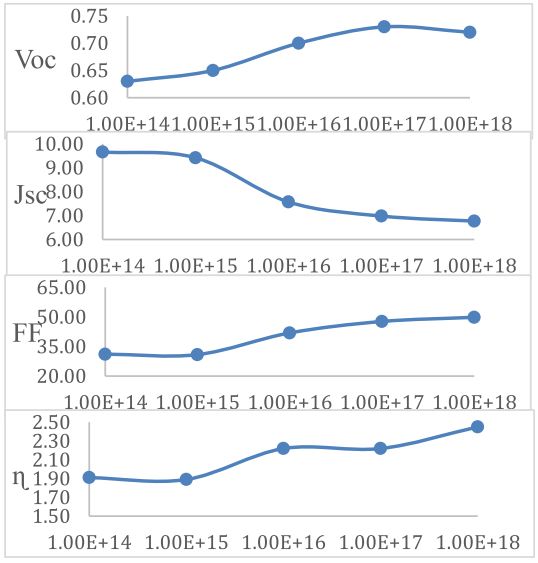

Fig. 11. Cell parameters as a function of concentration doping CFTS layer.

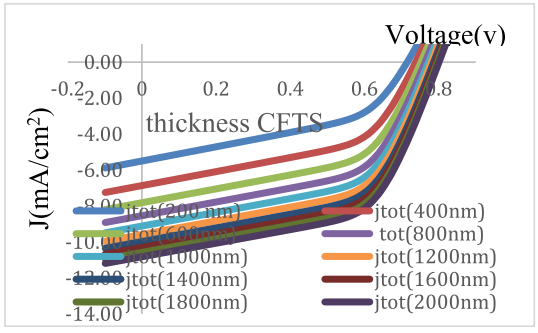

Fig. 12. Current as a function of voltage for different thicknesses values of the absorbing layer.

thickness of the absorbing layer. And the reason is that the increase of the thickness leads to an increase of photons that have less energy than the forbidden energy gap [27] and the largest thickness of 2 μm was chosen and Fig. 12 shows the

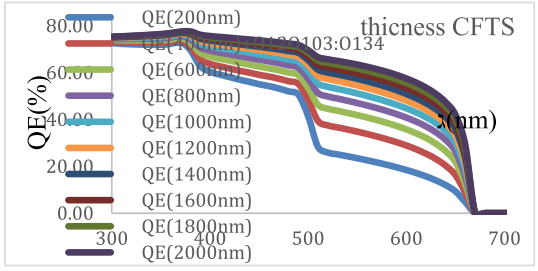

Fig. 13. Quantitative efficiency as a function of wavelength for different thicknesses values of the absorbing layer.

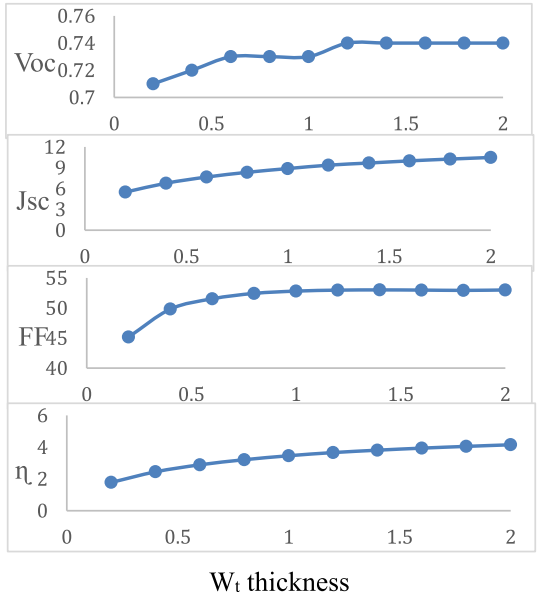

Fig. 14. Cell parameters as a function of the thickness of CFTS layer.

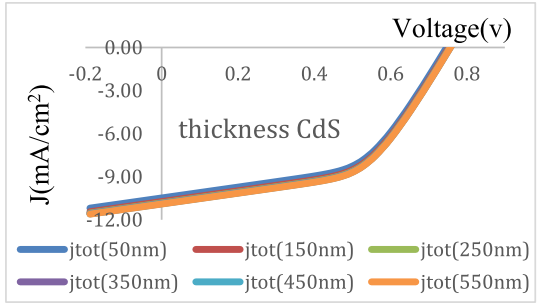

Fig. 15. Current as a function of voltage for different thicknesses values of the buffer layer.

relationship of current with voltages for different thicknesses. Fig. 13 shows the relationship of quantum efficiency with wavelength for different thickness values. We note an increase in the quantitative efficiency with an increase in thickness, because increasing the thickness leads to an

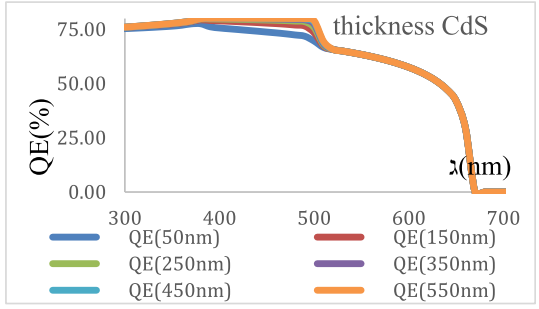

Fig. 16. Quantitative efficiency as a function of wavelength for different thicknesses values of the buffer layer.

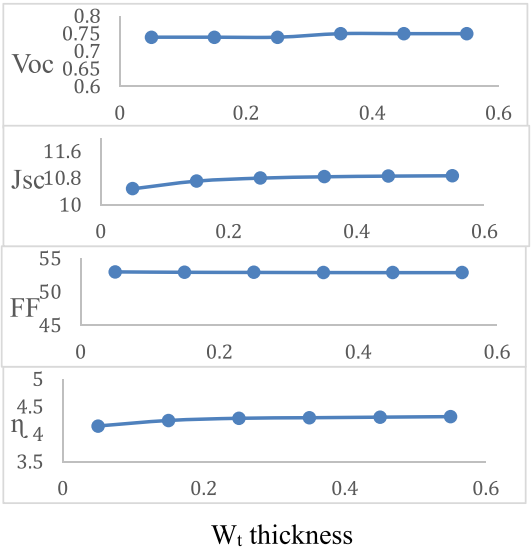

Fig. 17. Cell parameters as a function of CdS layer thickness.

Table 3. Theoretical cell and cell output after optimization.

Cell structure	Voc(v)	Jsc (mA/cm^2)	FF	η
AZO/i-ZnO/CdS/CFTS/Mo (theriacal)	0.55	6.2	39	1.35
AZO/i-ZnO/CdS/CFTS/Mo (optimization)	0.74	10.80	52.92	4.29

increase in the diffusion length and an increase in the life of minority carriers, which reduces the recombination [28] and Fig. 14 shows the cell parameters for different thicknesses.

3.4.2. Thickness of CdS

The buffer layer thickness provides a simple effect on the solar cell. Fig. 15 and Fig. 16 show the relationship of current with voltage, as well as the relationship of quantitative efficiency with the wavelength of different thicknesses of the CdS layer.

And Fig. 17 shows the cell parameter for different thicknesses of the buffer layer. There is a slight increase in efficiency from 4.15 to 4.29 and also a small

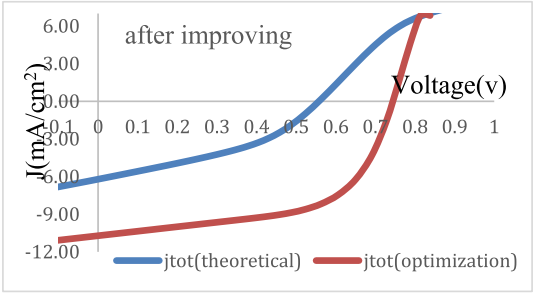

Fig. 18. The current is a function of the voltage of the theoretical cell before and after the optimization.

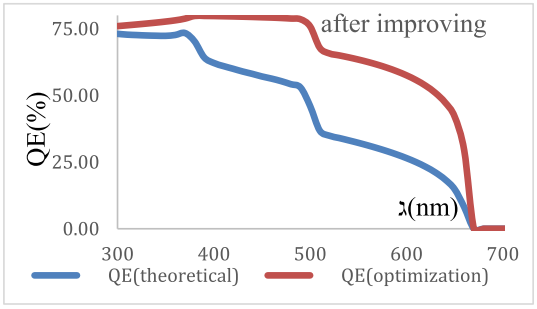

Fig. 19. The quantitative efficiency is a function of the wavelength of the theoretical cell before and after the optimization.

increase in the short circuit current and the stability of both the fill factor and the short circuit voltage.

3.5. Comparing the theoretical cell with the cell after optimization

Comparing the theoretical cell with the cell after optimization, note that the cell performance increased and Table 3 shows the parameters of the cell before and after the improvement. We notice that the cell efficiency increased from 1.35 until it became 4.29 and Fig. 18 shows the relationship of current with voltage and the extent of improvement in the cell. Fig. 19 shows the relationship of quantitative efficiency with the wavelength of the theoretical cell and the cell after optimization.

4. Conclusion

The AZO/i-ZnO/CdS/CFTS solar cell was simulated using the SCAPS program and compared with the experimental cell, where the parameters of the experimental research were entered and supplemented by other researches. It was found that there is a good match between the experimental and theoretical work after interring surface defects of CFTS/CdS and defects of the CFTS absorption layer. To improve the experimental cell, we changed the concentration of the accepter and the thickness of the absorbent layer. We noticed that the increase in doping and thickness increases the efficiency of the cell, due to the decrease in the saturation current and the increase in the open-circuit voltage. Then we made a change in the donor concentration and thickness of the buffer layer, and we noticed an increase in efficiency, but the effect of thickness was little, so the cell efficiency reached 4.29.

Acknowledgments

The search is not supported by any institution because the SCAPS program used in the search is available for free.

References

[1] F. Birol, Key world energy statistics, International Energy Agency (IEA), 2017, p. 3.

[2] O. Skhouni, A. El Manouni, H. Bayad, B. Mari, Boosting the performance of solar cells with intermediate band Absorbers the case of ZnTe:O, J. Energy Power Eng. 11 (2017) 417–426.

[3] C.W. Huang, S. S Kuo, C.L. Hsin, Electron-beam-induced phase transition in the transmission electron microscope: the case of VO_2 (B), Cryst. Eng. Comm. 20 (43) (2018) 6857–6860.

[4] F.K. Konan, B. Hartiti, Numerical simulations of highly efficient Cu2FeSnS4 (CFTS)-based solar cells, Int. J. Renew. Energy Res. (IJRER) 9 (2019) 1865–1872.

[5] H. Guo, Y. Li, X. Guo, N. Yuan, J. Ding, Effect of silicon doping on electrical and optical properties of stoichiometric Cu_2ZnSnS_4 solar cells, Physica B: Conden. Matter 531 (2018) 9–15.

[6] D.B. Mitzi, O. Gunawan, T.K. Todorov, D.A.R. Barkhouse, Prospects and performance limitations for Cu–Zn–Sn–S–Se photovoltaic technology, Phil. Trans. Roy. Soc. A: Math. Phys. Eng. Sci. 371 (2013) 1996, 20110432.

[7] C. Steinhagen, M.G. Panthani, V. Akhavan, B. Goodfellow, B. Koo, B.A. Korgel, Synthesis of Cu_2ZnSnS_4 nanocrystals for use in low-cost photovoltaics, J. Am. Chem. Soc. 131 (2009) 12554–12555.

[8] K. Kim, W.N. Shafarman, Alternative device structures for CIGS-based solar cells with semi-transparent absorbers, Nano Energy 30 (2016) 488–493.

[9] G.S.D. Babu, X.S. Shajan, S. Alwin, V. Ramasubbu, G.M. Balerao, Effect of reaction period on stoichiometry, phase purity, and morphology of hydrothermally synthesized Cu_2NiSnS_4 Nanopowder, J. Electron Mater. 47 (2018) 312–322.

[10] A.S. Oreshonkov, E.M. Roginskii, V.V. Atuchin, New candidate to reach Shockley–Queisser limit: the DFT study of orthorhombic silicon allotrope Si (oP32), J. Phys. Chem. Solid. 137 (2020) 109219.

[11] X. Meng, H. Deng, J. Tao, H. Cao, X. Li, L. Sun, J. Chu, Heating rate tuning in structure, morphology and electricity properties of Cu_2FeSnS_4 thin films prepared by sulfurization of metallic precursors, J. Alloys Compd. 680 (2016) 446–451.

[12] A. Le Donne, V. Trifiletti, S. Binetti, New earth-abundant thin film solar cells based on chalcogenides, Front. Chem. 7 (2019) 297.

[13] X. Meng, H. Deng, J. He, L. Zhu, L. Sun, P. Yang, J. Chu, Synthesis of $Cu_2FeSnSe_4$ thin film by selenization of RF magnetron sputtered precursor, Mater. Lett. 117 (2014) 1–3.

[14] W. Eisele, A. Ennaoui, P. Schubert-Bischoff, M. Giersig, C. Pettenkofer, J. Krauser, F. Karg, XPS, TEM and NRA investigations of Zn(Se,OH)/$Zn(OH)_2$ films on Cu(In,Ga)$(S,Se)_2$ substrates for highly efficient solar cells, Sol. Energy Mater. Sol. Cell 75 (2003) 17–26.

[15] H.B. Michaelson, The work function of the elements and its periodicity, J. Appl. Phys. 48 (1977) 4729–4733.

[16] S.A. Vanalakar, P.S. Patil, J.H. Kim, Recent advances in synthesis of Cu_2FeSnS_4 materials for solar cell applications: a review, Sol. Energy Mater. Sol. Cell 182 (2018) 204–219.

[17] F. Baig, Numerical analysis for efficiency enhancement of thin film solar cells, Doctoral dissertation, Universitat Politècnica de València, 2019.

[18] O. Skhouni, A. El Manouni, B. Mari, H. Ullah, Numerical study of the influence of ZnTe thickness on CdS/ZnTe solar cell performance, Eur. Phys. J. Appl. Phys. 74 (2016) 24602–24611.

[19] K.Y. Hameed, B. Faisal, T. Hanae, S.B. Marí, B. Saira, K.N.A. Kaim, Modelling of novel-structured copper barium tin sulphide thin film solar cells, Bull. Mater. Sci. 42 (2019) 1–8.

[20] R. Ganvir, Modelling of the nanowire CdS-CdTe device design for enhanced quantum efficiency in Window-absorber type solar cells, thesis Master, University of Kentucky, 2016.

[21] A.H. Najim, A.N. Saleh, Study effect of window and BSF layers on the properties of the CZTS/CZTSe solar cell by SCAPS–1D, Tikrit J. Pure Sci. 24 (2019) 77–83.

[22] Y.H. Khattak, F. Baig, S. Ullah, B. Marí, S. Beg, H. Ullah, Numerical modeling baseline for high efficiency (Cu_2FeSnS_4) CFTS based thin film kesterite solar cell, Optik 164 (2018) 547–555.

[23] L. Et-taya, T. Ouslimane, A. Benami, Numerical analysis of earth-abundant $Cu_2ZnSn(SxSe1\text{-}x)_4$ solar cells based on Spectroscopic Ellipsometry results by using SCAPS-1D, Solar Energy 201 (2020) 827–835.

[24] M. Courel, F.A. Pulgarín-Agudelo, J.A. Andrade-Arvizu, O. Vigil-Galán, Open-circuit voltage enhancement in CdS/$Cu_2ZnSnSe_4$-based thin film solar cells: a metal–insulator–semiconductor (MIS) performance, Sol. Energy Mater. Sol. Cell 149 (2016) 204–212.

[25] M. Courel, J.A. Andrade-Arvizu, O. Vigil-Galán, Loss mechanisms influence on Cu_2ZnSnS_4/CdS-based thin film solar cell performance, Solid State Electron. 111 (2015) 243–250.

[26] A. Martin, Crane translation by Dr. Y.M Hassan, Solar cells principles of work, technology and system Applications, Baghdad National Library, 1989 (In Arabic).

[27] S.R. Nalage, M.A. Chougule, P.B. Sen, S. Joshi, V.B. Patil, Sol–gel synthesis of nickel oxide thin films and their characterization, Thin Solid Films 520 (2012) 4835–4840.

[28] G. Azzouzi, Study of silicon solar cells performances using the impurity photovoltaic effect, Doctoral dissertation, University Ferhat Abbas–Setif, 2014.